BIOCHEMISTRY
including biophysical chemistry & molecular biology

Article

pubs.acs.org/biochemistry

A Molecular Dynamics and Quantum Mechanics/Molecular Mechanics Study of the Catalytic Reductase Mechanism of Methionine Sulfoxide Reductase A: Formation and Reduction of a Sulfenic Acid

Hisham M. Dokainish and James W. Gauld*

Department of Chemistry and Biochemistry, University of Windsor, Windsor, Ontario N9B 3P4, Canada

Supporting Information

ABSTRACT: The catalytic mechanism of MsrA in *Mycobacterium tuberculosis*, in which *S*-methionine sulfoxide (Met-O) is reduced to methionine (Met), has been investigated using docking, molecular dynamics (MD) simulations, and ONIOM (quantum mechanics/molecular mechanics) methods. In addition, the roles of specific active site residues, including an aspartyl (Asp87) near the recycling cysteine, tyrosyls (Tyr44 and Tyr92), and glutamyl (Glu52), have been examined, as well as the general effects of the protein and active site on the nature and properties of mechanistic intermediates. The mechanism is initiated by the transfer of a proton from the catalytic cysteine's thiol (Cys13SH) via a bridging water to the R group carboxylate of Glu52. The now anionic sulfur of Cys13 nucleophilically attacks the substrate's sulfur with concomitant transfer of a proton from Glu52 to the sulfoxide oxygen, generating a sulfurane. The active site enhances the proton affinity of the sulfurane oxygen, which can readily accept a proton from the phenolic hydroxyls of Tyr44 or Tyr92 to give a sulfonium cation. Subsequently, Asp87 and the recycling cysteine (Cys154) can facilitate nucleophilic attack of a solvent water at the Cys13S center of the sulfonium to give a sulfenic acid (Cys13SOH) and Met. For the subsequent reduction of Cys13SOH with intramolecular disulfide bond formation, Asp87 can help facilitate nucleophilic attack of Cys154S at the sulfur of Cys13SOH by deprotonating its thiol. This reduction is found likely to occur readily upon suitable positioning of the active site hydrogen bond network and the sulfur centers of both Cys13 and Cys154. The calculated rate-limiting barrier is in good agreement with experiment.

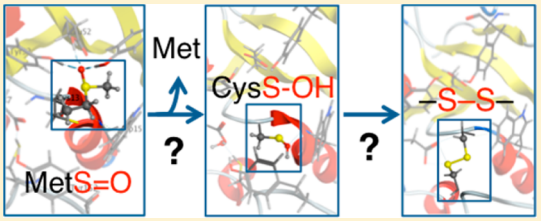

Of the standard 20 genetically encoded amino acids, methionine (Met) is one of the most easily oxidized.[1] In particular, oxidation at its R group sulfur can lead to formation of methionine sulfoxide (Met-O).[1] Remarkably, Met-O can be reduced to give Met.[2] This uncommon amino acid redox chemistry has increasingly been shown to be critical for many biological processes, including protein regulation, the calcium-induced signal transduction pathway, and immune responses.[1,3−6] However, such post-translational modifications induced by oxidative stress are also known to be involved in aging and age-related diseases, including cancer and Alzheimer's disease.[7−9]

Methionine sulfoxide reductases (Msr's) make up a family of ubiquitous enzymes that reduce Met-O to Met.[10,11] These enzymes have been shown to be important, for example, in cellular responses to oxidative stress[12−14] and bacterial virulence[15,16] and against amyloid β-protein toxicity.[17] There are two main classes of Msr's, A and B, which are stereospecific for the *S*- and *R*-Met-O epimers, respectively.[18,19] Both classes are thought to utilize the same overall reaction despite having quite distinct active site compositions and being structurally unrelated.[20] The few shared similarities include an active site cysteinyl and tryptophanyl that are thought to act as a nucleophile and help orient the substrate, respectively. In addition, both have several hydrogen bond donors that interact with the Met-O sulfoxide oxygen. However, the nature of these donors differs. MsrB has multiple ionizable and polar residues,[21] while MsrA contains two tyrosyls and a glutamyl residue.[22] In vitro studies[2] of recombinant MsrA have shown it to be 10-fold more active than MsrB. Furthermore, for several species, it has been found that knocking it out enhances their susceptibility to oxidative stress,[23−25] while its overexpression results in longer lifespans.[26,27] Meanwhile, its downregulation in human breast cancer cells increased the disease's aggressiveness both in vivo and in vitro.[28]

Several experimental kinetic studies of MsrA have examined the possible roles of various active site amino acid residues. For instance, substitution of Cys51 of *Escherichia coli* MsrA by serine deactivated the enzyme, thus confirming its essential catalytic role.[29] Similarly, substitution of the active site glutamyl (Glu94 in *Neisseria meningitidis*), thought to be important both in the activation of Cys51 and as the donor of a proton to the substrate, by alanine drastically reduced the rate of catalysis 36500-fold.[22] In contrast, mutation of either active site tyrosyl

Received: August 30, 2012
Revised: February 12, 2013
Published: February 18, 2013

   dx.doi.org/10.1021/bi301168p | *Biochemistry* 2013, 52, 1814−1827

Scheme 1. Proposed[30,31] Reductase Mechanisms for MsrA via (A) a Sulfenic Acid Intermediate or (B) Direct Attack

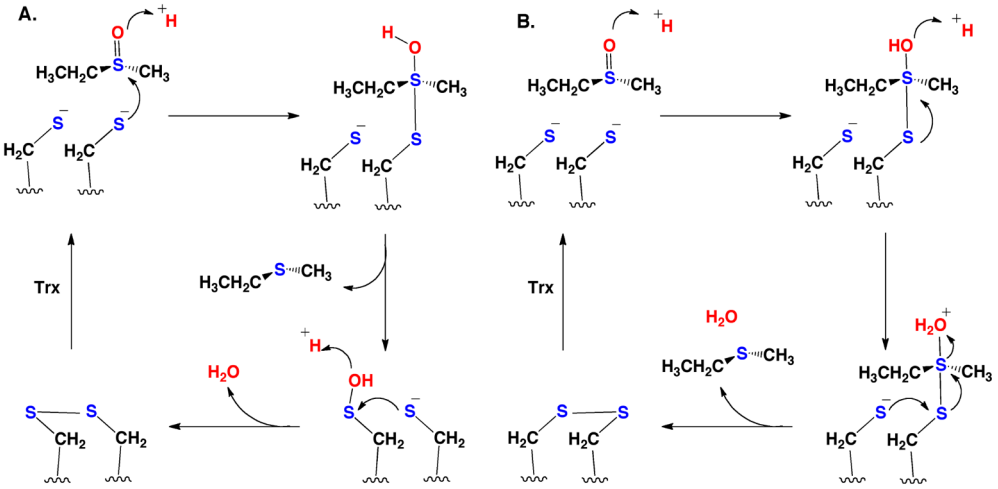

Scheme 2. Proposed[18] Catalytic Reductase Mechanism for MsrA Involving Formation of a Sulfenic Acid Intermediate via Attack of a Solvent Water at the Catalytic Cysteine's Sulfur Center

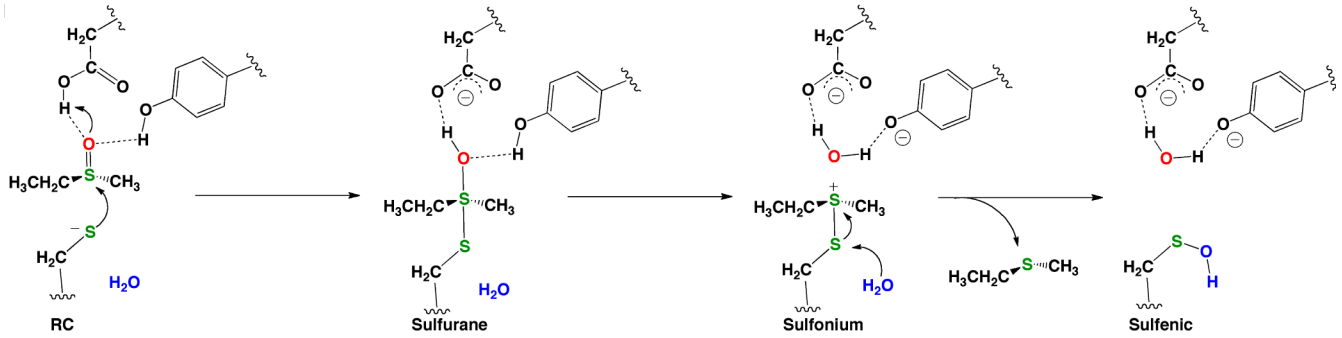

(Tyr82 or Tyr134 in *N. meningitidis*) to Phe appeared to have little effect on the rate of reaction.[22] However, simultaneous substitution of both with Phe decreased the catalytic rate significantly by ~10000-fold.[22] In addition, using chemical probes and mass spectrometry, a catalytic cysteine-derived sulfenic acid was detected in a wild-type MsrA from *E. coli*.[29] The ionization states of Cys51 (the catalytic cysteine) and a second active site cysteine, Cys198, known as the recycling cysteine, have also been experimentally measured. In particular, it was observed that upon substrate binding the pK_a of Cys51 was reduced significantly from 9.5 to 5.7 in *N. meningitidis*.[22] However, it was decreased only to 8.0 if Glu94 was replaced with Gln or if both Tyr82 and Tyr134 were replaced with Phe. This was suggested to indicate that these three residues are important for polarizing the sulfoxide S═O bond, which also leads to a decrease in the pK_a of Cys51.[22]

On the basis of these and related experimental studies, several possible catalytic mechanisms for MsrA and by extension Msr's in general were proposed and are summarized in Scheme 1.[18,30,31] Specifically, upon activation of Cys51 by some as yet unclear process to give the Cys51S$^-$ thiolate, proposed mechanisms A and B in Scheme 1 commonly begin with formation of a sulfurane via nucleophilic attack of Cys51S$^-$ at the Met-O sulfur.[32] However, two alternate mechanisms were suggested for the subsequent reactions of the sulfurane. (A) It undergoes a 1,2-shift of the sulfurane's OH group from the substrate sulfur to the adjacent Cys51 sulfur to give the sulfenic acid Cys51SOH and the desired Met product, or (B) it is protonated at its oxygen to give a sulfonium. In the former mechanism, the resulting catalytic cysteine-derived sulfenic acid intermediate readily reacts with the recycling cysteine, which itself has been activated and is in its thiolate form, to give an intramolecular disulfide bond. In contrast, in the latter proposed mechanism (B), the recycling cysteine thiolate directly attacks the Cys51S center of the sulfonium to give an intramolecular disulfide bond and the reduced Met product, i.e., without formation of the sulfenic acid.[14] In both cases, the active site is then ultimately regenerated via reduction of the disulfide bond by thioredoxin (Trx).[33]

However, more recently, Lim et al.[18] using mass spectrometry and isotope labeling identified peptide modifications formed during the catalytic mechanism of mouse MsrA. To prevent other modifications such as disulfide bond formation, they mutated Cys107, Cys218, and Cys227 to serine. They observed that the catalytic cysteine was converted to a sulfenic acid (CysSOH) during the course of the mechanism. Importantly, and in contrast to what was previously proposed, the CysSOH oxygen was not derived from the initial Met-O substrate but instead from the aqueous solvent. Consequently, they proposed a modified mechanism for MsrA involving sulfonium and sulfenic acid intermediates highlighted in Scheme 2.

Computationally, there have been very few studies of the catalytic mechanism of Msr's. Recently, Thiriot et al.[34] used a density functional theory (DFT) cluster approach to gain insights into the reductase mechanism of MsrA. Specifically, the

dx.doi.org/10.1021/bi301168p | *Biochemistry* 2013, 52, 1814−1827

substrate was modeled with dimethyl sulfoxide (DMSO) and the R groups of active site residues Tyr134 and Tyr82, Glu94, and Cys51S$^-$ by phenol and water, CH_3S^-, and acetic acid, respectively. In addition, general environmental effects were included via use of a PCM solvation method with a dielectric constant (ε) of 2. Importantly, they showed that formation of a sulfonium intermediate may occur via nucleophilic attack of Cys51S$^-$ at the substrate's sulfur with stepwise protonation of its sulfoxide oxygen by Glu94 and Tyr134. Furthermore, a sulfenic acid intermediate was shown via calculation to have a quite low energy. Unfortunately, a reaction pathway between the sulfonium ion and sulfenic acid was not elucidated. However, they suggested it may involve dissociation of the sulfonium with the H_2O moiety released and then attack of the catalytic cysteinyl's sulfur to give a sulfenic acid.

Previously, we performed a computational investigation of the complete catalytic reductase mechanism of MsrB using a large DFT cluster model and with the general protein environment modeled by a PCM solvation method with an ε of 4, which is common in such approaches.[35] In particular, we showed that the mechanism may be initiated by nucleophilic attack of the catalytic Cys at the substrate's sulfur with concomitant transfer of a proton from a nearby histidyl residue to form a sulfurane. A sulfonium cation was then formed via transfer of a proton from a second histidyl residue onto the sulfurane's oxygen. However, within the computational model used, two possible enzymatically feasible mechanisms were then obtained by which the Met product could be formed: (i) direct attack of the recycling cysteine thiolate at the sulfonium's catalytic cysteinyl sulfur or (ii) via a sulfenic acid intermediate. The latter was found not to be feasible via intramolecular rearrangement of the sulfurane as previously suggested. Instead, it required a solvent water to attack the sulfonium's catalytic cysteinyl sulfur as experimentally observed in MsrA.[18]

A clearer elucidation of the catalytic mechanism of Msr's is central to an improved understanding of their role in aging, oxidative stress, and other important physiological processes. In addition, because of their use of a diverse variety of sulfur compounds and chemistry, they represent a tremendous opportunity to obtain greater insights into the important area of sulfur biochemistry, in particular that of highly reactive species such as sulfenic acids. We have thus performed a detailed systematic computational investigation of the catalytic mechanism of MsrA. More specifically, we have complementarily applied docking, molecular dynamics (MD) simulations, and an extensive ONIOM quantum mechanics/molecular mechanics (QM/MM) approach to investigate activation of the catalytic cysteinyl and the subsequent reductase mechanism that leads to formation of Met and the intramolecular disulfide bond.

COMPUTATIONAL METHODS

Docking and MD Studies. These calculations were performed using the Molecular Operating Environment (MOE).[36] The X-ray crystal structure [Protein Data Bank (PDB) entry 1NWA] of MsrA from *Mycobacterium tuberculosis* ($MsrA_{Mtb}$) complexed with protein-bound methionine was used as a template for docking.[37] The substrate and all crystal structure waters were removed then the substrate methionine sulfoxide (Met-O) docked into its active site, where all residues within the first interaction shell of the catalytic cysteine (Cys13) were considered as in the active site. The London dG scoring function was used in conjunction with a force field refinement method to obtain the top 30 scoring structures. These were visually examined to choose the most suitable starting structure for further calculations. A molecular dynamics (MD) simulation was then performed on the chosen structure to allow for thermal relaxation. More specifically, the enzyme–substrate complex was spherically solvated up to 15 Å from the substrate. Then MD simulations were performed for 1 ns using a time step of 2 fs in a same manner that has been previously described.[38] The structures generated during the simulation were analyzed and clustered according to the distance between the sulfurs of the catalytic cysteine and substrate into 10 clusters. As shown in Figure S1 of the Supporting Information, the overlay of the 10 average structures of the generated clusters shows similar interactions; furthermore, the root-mean-square deviation (rmsd) of the QM region moieties (QM-rmsd) of the 10 structures was 0.12 Å, indicating a very consistent structure. The average structure of the most populated cluster was then optimized using the AMBER99 force field,[39] and the resulting structure (structure **A′**) was used to construct a QM/MM chemical model to examine the catalytic mechanism of MsrA up to and including formation of a sulfenic acid intermediate.

A second MD simulation was performed to model possible rearrangements in the active site upon sulfenic acid formation. As in the protocol detailed above, the X-ray crystal structure of PDB entry 1NWA was modified to remove the substrate and all crystallographic waters. The catalytic cysteine was then modified to form a sulfenic acid (CysSOH) and the resulting intermediate spherically solvated up to 15 Å from the sulfur of the CysSOH moiety. The complex was equilibrated for 0.5 ns followed by a 1 ns production run as previously described.[40] The S–O bond of the CysSOH moiety was constrained to its optimized length as obtained at the B3LYP/6-31G(d) level of theory. Partial charges for the sulfenic acid were also obtained via a Mulliken population analysis of IC3 performed below the QM/MM level of theory. The resulting structures obtained were cluster-analyzed on the basis of the sulfenic acid hydrogen bonding network into 10 clusters (see above). Similarly, the 10 average structures were overlaid (Figure S2 of the Supporting Information) and analyzed and found to have a QM-rmsd of 0.24 Å. Again, the average structure of the most populated cluster was chosen and optimized using the AMBER99 force field.[39] The resulting complex, structure **B′**, was used to construct a QM/MM chemical model to examine the catalytic mechanism of MsrA for formation of the final product from the sulfenic acid intermediate.

QM/MM Models and Calculations. All QM/MM calculations were performed within the ONIOM formalism[41] using the Gaussian 09[42] suite of programs. Density functional theory method B3LYP, a combination of Becke's three-parameter exchange functional[43] and Lee, Yang, and Parr's correlation functional,[44] was used for the high-layer (QM), while the AMBER96[45] force field was used for the low-layer (MM) parametrization. Optimized geometries (the default convergence criteria of Gaussian 09[42] were used throughout) were obtained using the 6-31G(d) basis set for the high-layer and within the mechanical embedding (ME) formalism, i.e., at the ONIOM(B3LYP/6-31G(d):AMBER96)-ME level of theory. Frequency calculations were also obtained at this same level of theory to characterize the nature of the stationary points obtained (i.e., minima or transition structures) and to calculate Gibbs energy corrections (ΔG_{corr}). The single imaginary and first real frequencies for the optimized TSs are

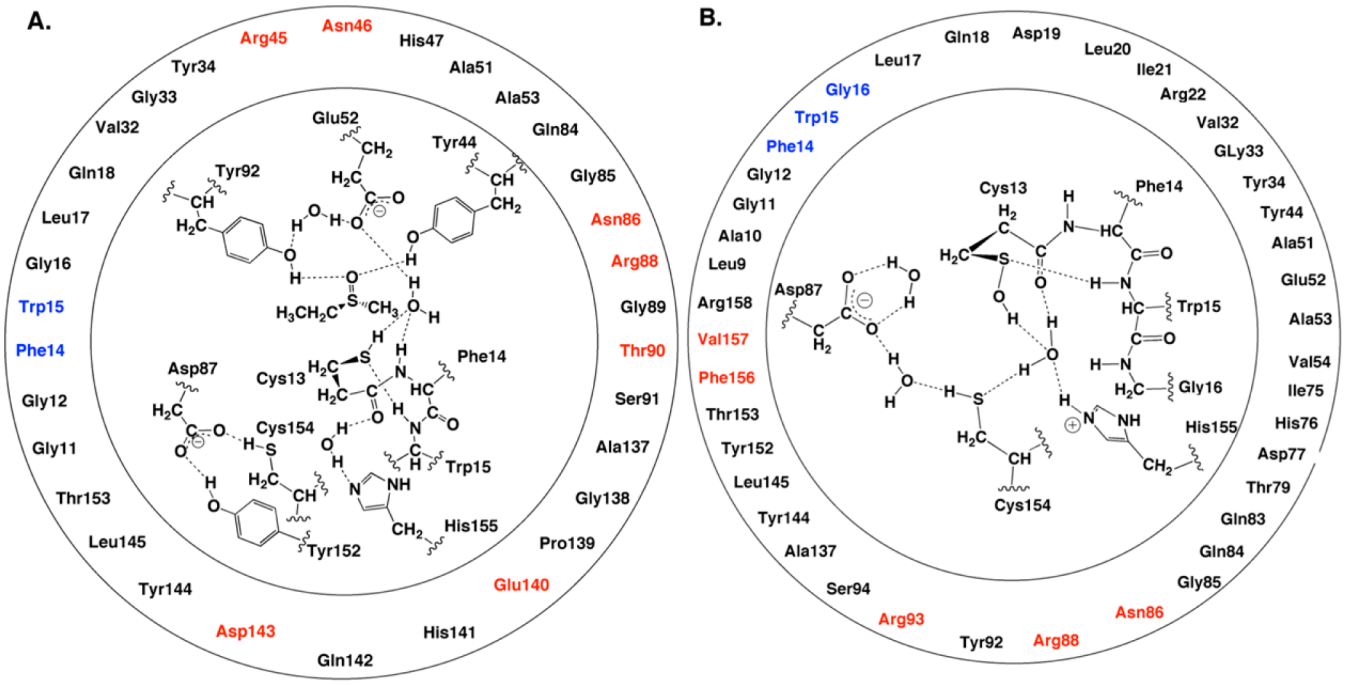

Figure 1. QM/MM models used to examine the catalytic mechanism of MsrA for (A) formation of an enzyme-derived sulfenic acid intermediate from the initial enzyme−substrate complex and (B) reaction of the enzyme-derived sulfenic acid intermediate to give the final products. The inner circles represent the QM layer, while the outer circles represent the MM layer. Color key for MM residues: black for those included in their entirety, red for cases in which the R group is replaced with hydrogen, and blue for cases in which the R group is included in the MM layer while the backbone is in the QM layer.

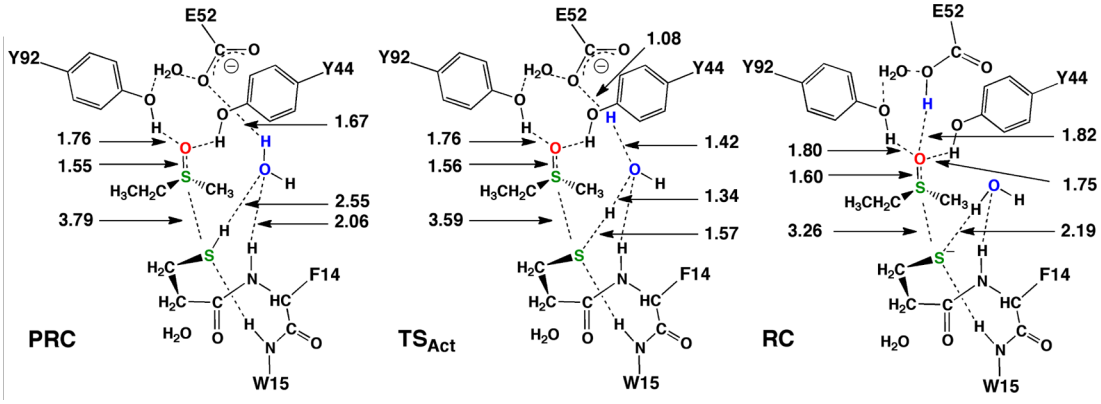

Figure 2. Schematic illustration of the optimized structures of the prereactive complex (**PRC**), activated reactive complex (**RC**), and transition structure ($\mathbf{TS_{Act}}$) for their interconversion. For the sake of simplicity, only selected residues, functional groups, and bond lengths (angstroms) are shown.

reported in Table S2 of the Supporting Information. Relative energies were then obtained via single-point energy calculations at the ONIOM(B3LYP/6-311+G(2df,p):AMBER96) level of theory within the electrostatic embedding (EE) formalism on the optimized structures described above, and with inclusion of the appropriate ΔG_{corr}. All atoms in the QM layer were unfixed, while for the MM layer, only the C_α centers were kept fixed at their final MD positions. This and similar QM/MM approaches have been successfully used to explore a range of enzymatic systems.[46−52]

The chemical models used were obtained by truncating structures **A′** and **B′** to include only those residues in the first and second shells centered on the sulfur of the catalytic cysteine and where appropriate the substrate. The two resulting active sites models, A and B, allowed us to more effectively consider the different stages in the overall mechanism and are shown in Figure 1. More specifically, models A and B were used to investigate possible catalytic mechanisms of MsrA resulting in (i) formation of an enzyme-derived sulfenic acid intermediate and (ii) conversion of a sulfenic acid intermediate to the final products, respectively. In model A, the Met-O substrate was modeled by ethylmethyl sulfoxide. It should be noted that in model A (Figure 1A) the catalytic and recycling cysteinyls (Cys13 and -154), three tyrosyls (Tyr92, -44, and -152), three charged residues (Glu52, Asp87, and His155), three H_2O molecules, and the backbone of Trp15, Phe14, and Cys154 were included in the QM layer. The R groups of Phe14 and Trp15 were kept in the low (MM) layer as DFT does not take into account van der Waals interactions that are important for their interactions with the Met-O substrate.[53] It is worth noting

dx.doi.org/10.1021/bi301168p | *Biochemistry* 2013, 52, 1814−1827

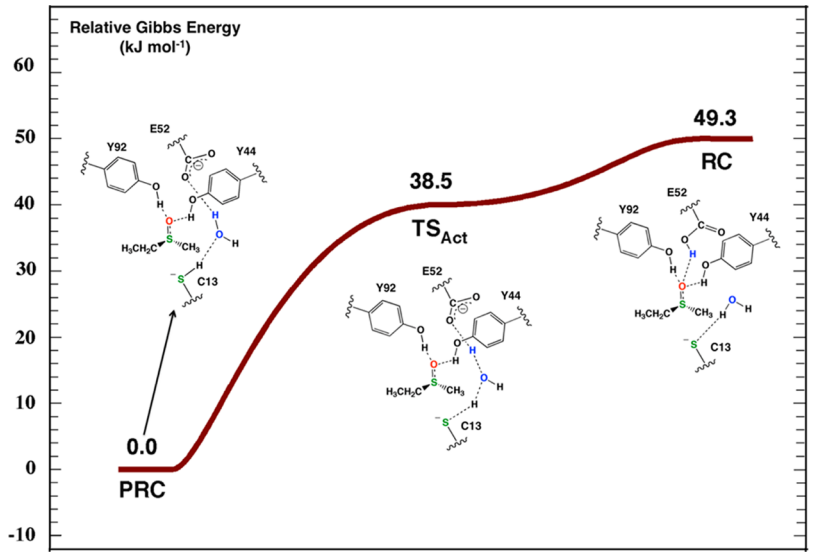

Figure 3. Free energy surface obtained (see Computational Methods) for activation of the catalytic cysteine (Cys13) by proton transfer via a bridging H_2O to the active site glutamate (Glu52).

that several QM/MM models that contained a smaller QM region were also tested, e.g., lacking residues near the catalytic and recycling catalytic cysteinyls. However, these were found to not adequately describe the chemistry of the reactions that would likely occur as part of the mechanism. For model B (Figure 1B), the QM layer included the catalytic and recycling cysteinyls (Cys13 and -154), two charged residues (Asp87 and His155), three H_2O molecules, and the backbone of Trp15 and Phe14.

RESULTS AND DISCUSSION

Substrate Binding and Activation of the Catalytic Cysteine. As noted in the introductory section, all previously proposed mechanisms involve nucleophilic attack of the sulfur of the thiolate form of the catalytic cysteine (Cys13 in $MsrA_{Mtb}$) at the sulfur center (S_{sub}) of the Met-O substrate.[18,31,33] For this to occur, however, Cys13 must be activated by deprotonation of its thiol. Indeed, as noted previously, it has been shown experimentally[22] that in the absence of the substrate the pK_a of the thiol of the catalytic cysteine is 9.5 but decreases to 5.7 upon substrate binding. X-ray crystal structures of MsrA's from different species have revealed that there is no basic residue in the proximity of the catalytic cysteine,[22] the closest being a glutamyl (Glu52 in $MsrA_{Mtb}$) ~5 Å away.[37] Nevertheless, Glu52 has been suggested to play a role in activating Cys13 and lowering the pK_a of its thiol.[22]

In the optimized structure of the prereactive complex (**PRC**) in which the substrate is bound within the active site and Cys13 is neutral, a water molecule forms a hydrogen bond bridge between the Cys13 thiol and the R group carboxyl of Glu52 with distances of 2.55 and 1.67 Å, respectively (Figure 2). In the MD simulations on the PRC complex, a water was also observed to consistently be similarly positioned and hydrogen-bonded (Figure S2 of the Supporting Information). Meanwhile, the backbone amide -NH- moiety of W15 forms a weak hydrogen bond with the Cys13SH sulfur with a length of 3.07 Å.[54] Meanwhile, the substrate's sulfoxide oxygen (O_{sub}) is observed to form shorter, stronger hydrogen bonds with the phenol hydroxyls of Tyr92 and Tyr44 with lengths of 1.76 and 1.78 Å, respectively. As a result, the substrate's $S_{sub}{=}O_{sub}$ bond becomes markedly longer upon binding by 0.08 Å, to 1.55 Å (Table S1 of the Supporting Information). It is noted that the distance between the sulfurs of Cys13 and the substrate, r(Cys13S···S_{sub}), is quite long in **PRC** (3.79 Å).

The structure and, in particular, the hydrogen bond network within **PRC** suggest that Cys13SH may be able to transfer a proton via a bridging H_2O onto the R group carboxylate of Glu52. At the B3LYP/6-31G(d) level of theory, the proton affinities (PAs) of methylthiolate and acetate, models of the ionized R groups of cysteine and glutamate, are calculated to lie just 34.3 kJ mol^{-1} apart, with the former being the more basic (Table S1 of the Supporting Information). Indeed, Cys13SH is able to formally transfer a proton through a H_2O onto the carboxylate of the Glu residue. This step proceeds via $\mathbf{TS_{Act}}$ at a cost of just 38.5 kJ mol^{-1} (Figure 3). The slightly lower relative energy of $\mathbf{TS_{Act}}$ (10.8 kJ mol^{-1}) with respect to that of **RC** is an artifact of the use of free energy corrections and indicates that at 298 K **RC** can effectively convert back to **PRC** without a barrier. It indicates that the reverse reaction, i.e., transfer of a proton from Glu51COOH via a water to Cys13S$^-$, effectively occurs without a barrier. As can be seen in the structure of $\mathbf{TS_{Act}}$ (Figure 2), the thiol's proton lies approximately midway between the sulfur of Cys13 and the water's oxygen. Meanwhile, the water has almost wholly transferred its proton onto the glutamyl's carboxylate [r(Glu52COO$^-$···H−OH) = 1.08 Å]. This process may be facilitated by the moderately strong hydrogen bond between the H_2O and the backbone -NH- group of Phe14 in **PRC** and $\mathbf{TS_{Act}}$, which would help stabilize negative charge build-up on the water's oxygen and thus enhance the water's acidity. It should be noted that possible alternate mechanisms involving the transfer of a proton from Cys13SH via a H_2O (i) directly onto the sulfoxide oxygen of the Met-O substrate and (ii) to the glutamyl with concomitant nucleophilic attack of Cys13S$^-$ at the substrate's sulfur center were also examined. However, both mechanisms were found to be enzymatically unfeasible.

Two mechanistically relevant conformers of the reactive complex (**RC**) that differed only in the nature of the hydrogen bond formed by Glu52COOH were optimized. In one [**RC**′

dx.doi.org/10.1021/bi301168p | *Biochemistry* 2013, 52, 1814−1827

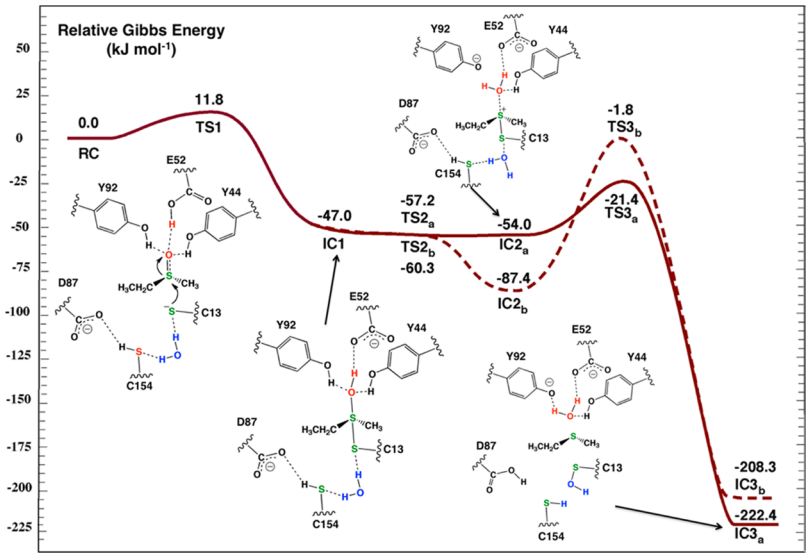

Figure 4. Free energy surface obtained (see Computational Methods) for formation of a sulfenic acid intermediate (Cys13SOH) involving proton donors (A) Glu52COOH and Tyr92OH and (B) Glu52COOH and Tyr44OH.

(not shown)], it is hydrogen bonded via the H_2O with the now deprotonated thiol of Cys13. However, a low-barrier rotation of the glutamyl's R group about its $C_\beta-C_\gamma$ bond, i.e., a change in its $C_\alpha-C_\beta-C_\gamma-O$ angle, from −86.6° to −62.4° gives rise to the alternate conformer **RC** shown in Figure 3, which is slightly higher in energy than **RC′** by 3.7 kJ mol^{-1} and just 49.3 kJ mol^{-1} higher in energy than **PRC**. In **RC**, the Glu52COOH group is now directly hydrogen bonded to the substrate's sulfoxide oxygen with an r(Glu52COOH···O_{sub}S) of 1.82 Å (Figure 2). The two phenol hydroxyls (Tyr92OH and Tyr44OH) also remain strongly hydrogen bonded to the substrate's sulfoxide oxygen with distances of 1.80 and 1.75 Å, respectively. As a result, the sulfoxide's $S_{sub}=O_{sub}$ bond has now become further elongated to 1.60 Å, increasing the negative charge on O_{sub} and enhancing the susceptibility of S_{sub} to nucleophilic attack. In addition, in **RC** the distance between the sulfurs of Cys13 and Met-O has decreased significantly by 0.53 Å, to 3.26 Å, such that they are now more suitably positioned for reaction.

Reduction of the Substrate with Formation of a Sulfenic Acid Intermediate. Following activation of the catalytic cysteine (Cys13) via the transfer of a proton to the carboxylate of the glutamate (Glu52) residue, the latter is then able to transfer the proton onto the substrate's sulfoxide oxygen. Concomitantly, the now anionic sulfur of Cys13 nucleophilically attacks the substrate's sulfoxide sulfur center, thus generating a sulfurane. This step proceeds via transition structure **TS1** with a quite low activation energy of only 11.8 kJ mol^{-1}, while the sulfurane intermediate formed, **IC1**, has a decidedly lower energy than **RC** by 47.0 kJ mol^{-1} (Figure 4).

The optimized structures of the reactant and product complex, intermediates, and transition structures obtained, with selected bond and interaction distances in angstroms, are schematically illustrated in Figure 5. As shown, in **TS1** the proton being transferred from the Glu52COOH group is roughly equidistant from the substrate's sulfoxide oxygen (O_{sub}) with r(Glu52COO···H$^+$) and r(O_{sub}···H$^+$) values of 1.23 and 1.22 Å, respectively. More importantly, however, the substrate's S−O bond has become markedly longer (1.74 Å), while the key Cys13S···S_{sub} distance has become significantly shorter by 0.51 Å, decreasing to 2.75 Å. In the sulfurane intermediate **IC1**, the S−O bond has become even longer (2.31 Å), while the Cys13S−S_{sub} disulfide bond has now formed as indicated by its length of 2.23 Å. It is noted that these bond lengths are in reasonable agreement with a sulfurane intermediate we obtained previously[35a] as part of a computational study of the mechanism of an MsrB using a DFT large active site chemical model approach. In contrast, the S−OH and S−S lengths are considerably longer and shorter, respectively, than those obtained by Thiriot et al.[34] in a computational study using more modest active site models. This suggests that the structure of the active site and its environment in MsrA and Msr's in general may act to help to stabilize a more polarized sulfurane intermediate.

In **IC1**, the sulfurane's oxygen now forms even shorter and stronger hydrogen bonds with the phenol hydroxyls of both Tyr44 and Tyr92 compared to that observed in **RC** with distances of 1.60 and 1.56 Å, respectively (Figure 5). As noted previously, experimental[22] mutation studies involving the two active site tyrosyls suggest that substitution of either alone reduces the rate of the reaction only slightly while mutation of both has a severe negative effect on the rate. Previous computational studies[34,35a] have suggested that the sulfurane hydroxyl (S_{sub}-O_{sub}H) can accept a proton from an acidic residue. This is likely facilitated in part by the sulfurane's O_{sub} basicity[35a] being greater than that of the sulfoxide oxygen in Met-O, which is likely further enhanced by the sulfurane's polarized nature within the active site. Thiriot et al.[34] suggested that one of the active site tyrosyls may be able to act as such an acid and protonate the sulfurane's O_{sub}H oxygen. Given the similar distances for the hydrogen bond interactions between O_{sub} and Tyr44OH and Tyr92OH (Figure 5), we considered the feasibility of either tyrosyl acting as the second mechanistic acid.

The phenol hydroxyl of Tyr92 is able to transfer its proton essentially without a barrier onto the sulfurane's oxygen, O_{sub}, via **TS2$_a$** to give sulfonium cation intermediate **IC2$_a$** (Figure 4). The latter lies slightly lower in energy than **IC1** by 7.0 kJ mol^{-1} (i.e., −54.0 kJ mol^{-1} with respect to **RC**). The fact that **TS2$_a$** (upon adding free energy corrections) is lower in energy than

dx.doi.org/10.1021/bi301168p | *Biochemistry* 2013, 52, 1814−1827

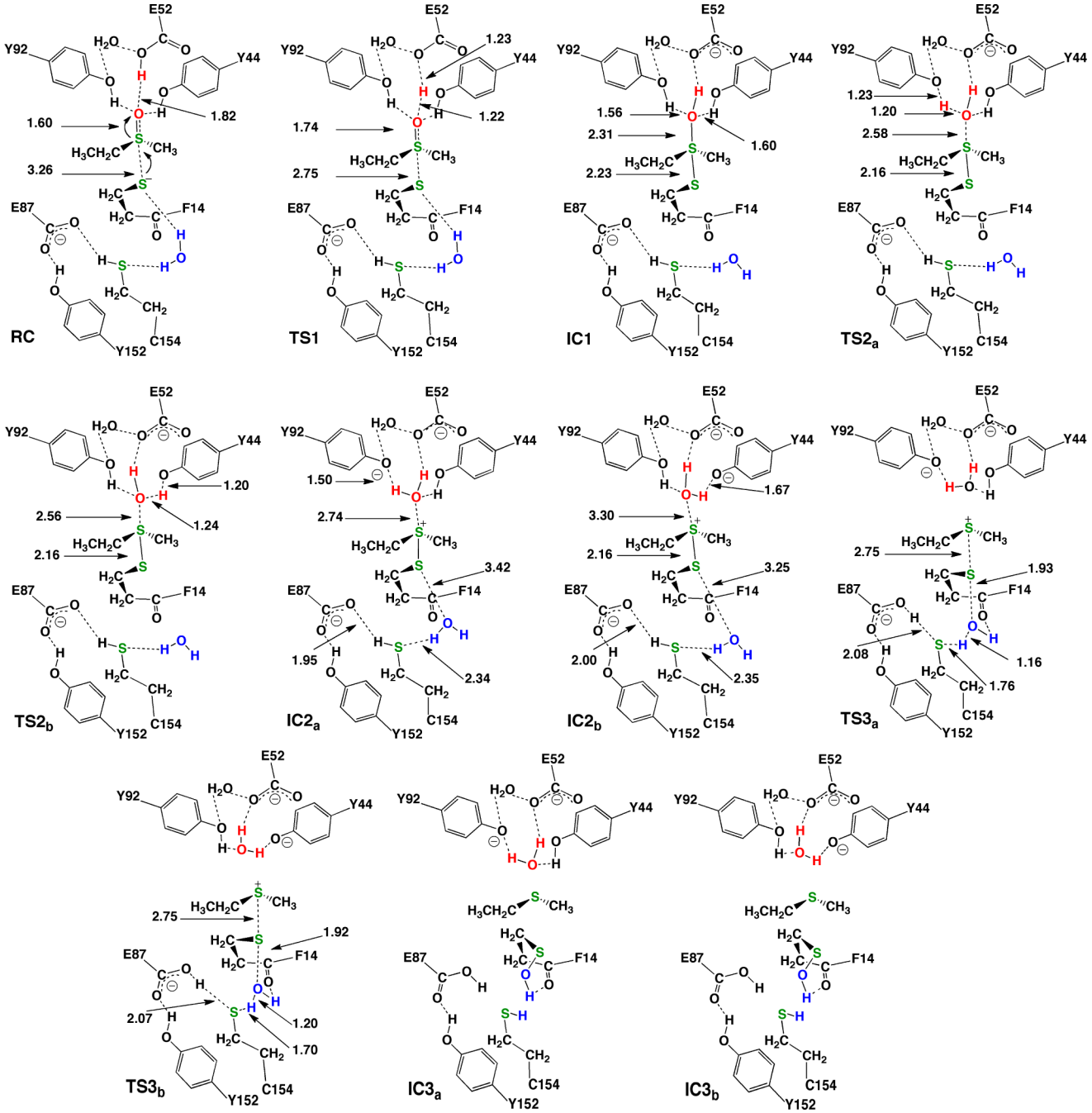

Figure 5. Schematic illustration of the optimized structures with selected bond lengths (in angstroms) of the minima and transition structures obtained for MsrA-catalyzed reduction of Met-O to Met with concomitant formation of an enzyme-derived sulfenic acid intermediate.

IC1 and **IC2**$_a$ suggests that these intermediates should be able to readily interconvert. In **TS2**$_a$, the proton is almost equidistant between the sulfurane and tyrosyl oxygens as indicated by the fact that the *r*(Tyr92O···H) and *r*(Tyr92O-H···O$_{sub}$) distances are 1.23 and 1.20 Å, respectively (Figure 5). In sulfonium complex **IC2**$_a$, the S$_{sub}$···OH$_2$ interaction has been effectively cleaved as indicated by its distance of 2.74 Å, while the Cys13S−S$_{sub}$ disulfide bond has become shorter [2.13 Å (Figure 5)].

Alternatively, Tyr44 can act as the second mechanistic acid. More specifically, it is able to transfer its phenolic proton onto the sulfurane's O$_{sub}$ via **TS2**$_b$ without a barrier (Figure 4). In contrast to that observed when Tyr92 acts as an acid, the resulting sulfonium complex formed, **IC2**$_b$, is calculated to have a decidedly lower energy than **IC1** by 40.4 kJ mol^{-1} (i.e., −87.4 kJ mol^{-1} with respect to that of **RC**). This greater stabilization of the sulfonium may reflect in part enhanced stabilization of the positive charge on the Cys13S−S$_{sub}$ disulfide by the now anionic phenol oxygen of Tyr44 at a distance of 2.80 Å. In contrast, the S$_{sub}$···OH$_2$ distance in **IC2**$_b$ is markedly longer than that in **IC2**$_a$, with a length of 3.30 Å (Figure 5).

In part on the basis of a previous computational study by Balta et al.,[55] Thiriot et al.[34] suggested that the sulfurane, upon protonation, may dissociate to a sulfonium cation and water molecule. The water moiety may then attack at the Cys13 sulfur center of the cationic disulfide to generate methionine

dx.doi.org/10.1021/bi301168p | *Biochemistry* 2013, 52, 1814−1827

(Met) and an enzyme-derived sulfenic acid (Cys13SOH). Indeed, for MsrA, a catalytic cysteine-derived sulfenic acid has been detected in mutant and wild-type enzymes using chemical probes and mass spectroscopy.[29] Unfortunately, they were unable to locate a pathway and barrier for this process. Also, it has previously been suggested that the sulfurane intermediate could undergo an analogous 1,2-sigmatropic shift of its $O_{sub}H$ group to generate Met and the sulfenic acid derivative.[14] However, we previously showed that the barrier for such a process was enzymatically unfeasible.[35a] Recently, experimental labeling studies have suggested that the oxygen of the sulfenic acid is in fact derived from the aqueous solvent and not the Met-O substrate.[18] Notably, in the optimized structures of both **IC2**$_a$ and **IC2**$_b$ (see Figure 5) and in an X-ray crystal structure of the wild-type enzyme, a H_2O is positioned within the active site and oriented such that its oxygen is directed toward the Cys13S center of the sulfonium disulfide moiety. Specifically, in **IC2**$_a$ and **IC2**$_b$, the distance between the water oxygen (O_w) and sulfonium's Cys13 sulfur center is 3.42 and 3.25 Å, respectively. Simultaneously, the water acts as the donor of a hydrogen bond to the sulfur of the recycling cysteine Cys154 with $r(OH_2\cdots SCys154)$ values of 2.34 and 2.35 Å in **IC2**$_a$ and **IC2**$_b$, respectively (Figure 5).

However, for nucleophilic attack of the water at Cys13S to occur, the H_2O needs either to be first deprotonated or to be able to donate a proton to a suitable base. In the model presented here, Cys154 has been modeled as neutral on the basis of its experimentally measured pK_a value of 9.5.[22] Thus, to be able to act as a suitable base, its thiol must itself be able to transfer its proton to a suitable base. Importantly, during the initial MD simulations of the initial active site-bound substrate complex (see Computational Methods), the thiol of Cys154 was observed to be consistently directly hydrogen bonded to the R group carboxylate of a spatially adjacent aspartyl (Asp87). In the QM/MM-optimized structures of both **IC2**$_a$ and **IC2**$_b$, the Cys154SH group forms a short and strong hydrogen bond to Asp87; $r(Cys154SH\cdots{}^{-}OOC\text{-}Asp87)$ = 1.95 Å. Consequently, the Cys154S−H bond itself is elongated, now with a length of 1.37 Å in both complexes compared to a length of 1.33 Å [at the B3LYP/6-31G(d) level of theory] in an isolated methylthiol. Thus, it appears that Cys154 may indeed be able to act as a suitable base to facilitate sulfenic acid formation. It is noted that within the active site region the only other residue that may be able to act as base is His155. However, the distance between the nearest nitrogen of its R group imidazole and H_2O is quite large (∼4.85 Å). Hence, it would seem less likely to be a suitable base to facilitate sulfenic acid formation.

In this study, for both situations in which Tyr92 or Tyr44 acts as the second mechanistic acid, the H_2O is able to directly attack at the Cys13 sulfur center of the sulfonium's disulfide bond. Importantly, this occurs with concomitant transfer of a proton from the attacking H_2O to the thiol of Cys154, which itself has transferred its proton to the adjacent R group carboxylate of Asp87. For the case in which Tyr92 acted as an acid, this step proceeds via **TS3**$_a$ at a cost of 32.6 kJ mol^{-1} with respect to **IC2**$_a$. In the resulting intermediate complex obtained, **IC3**$_a$, the desired methionine (modeled by ethylmethyl sulfide) product is bound within the active site. In particular, it is positioned such that its methyl is directed toward the R group of the active site tryptophanyl residue (Trp15). Furthermore, however, the catalytic cysteine (Cys13) has now been oxidized to a sulfenic acid (Cys13SOH). Thermodynamically, complex **IC3**$_a$ is significantly lower in energy than **IC2**$_a$ by 168.4 kJ mol^{-1}, which is −222.4 kJ mol^{-1} with respect to **RC**. Structurally, in **TS3**$_a$, it can be seen that the Cys154SH proton is essentially wholly transferred onto the carboxylate of Asp87; $r(Cys154S\cdots H^+)$ = 2.08 Å (Figure 5). In contrast, the proton being abstracted from the attacking H_2O lies between the Cys154S and O_w centers with distances of 1.76 and 1.16 Å, respectively (Figure 5). In contrast, for the pathway in which Tyr44 acted as an acid, this process occurs via **TS3**$_b$ with a markedly higher cost of 85.6 kJ mol^{-1} with respect to **IC2**$_b$ (Figure 4). In fact, the relative energy of **TS3**$_b$ is higher than that of **TS3**$_a$ by 19.6 kJ mol^{-1}. As obtained for **IC3**$_a$, in the resulting sulfenic acid-containing active site complex **IC3**$_b$, the desired ethylmethyl sulfide product is again positioned within the active site such that its methyl is oriented toward the R group of Trp15. In addition, **IC3**$_b$ also is considerably lower in energy than **IC2**$_b$ and **RC**, though now by 120.9 and 208.3 kJ mol^{-1}, respectively. Notably, while **IC3**$_b$ is slightly higher in energy than **IC3**$_a$ by 14.1 kJ mol^{-1} (see Figure 5), they can interconvert with each other. This could occur by a proton transfer via the H_2O that is simultaneously hydrogen bonded to the carboxylate of Glu52 and the phenolic oxygens of both Tyr92 and Tyr44 (see Figure 5). Structurally, **TS3**$_b$ is very similar to **TS3**$_a$ and hence is not discussed in detail here.

We have also considered the catalytic pathway from **RC** to **IC2** in which either Tyr92 or Tyr44 is substituted with a pheylalanyl (i.e., for mutated enzyme Y92F or Y44F). Structurally, mutating either tyrosyl leads to a strengthening of the Met-O S−O bond (i.e., decreased level of polarization of the S−O bond via hydrogen bonds with the Tyr-OH groups) and concomitantly longer −S−S− bond in the sulfurane (**IC1**). Furthermore, a slight reduction in the barrier for formation of **IC1** is observed; specifically, it decreases from 14.6 kJ mol^{-1} in the wild type to 12.8 and 4.6 kJ mol^{-1} in the Y44F and Y92F mutant enzymes, respectively (Figure S7 of the Supporting Information). It is noted that the magnitudes of these energy changes are within the expected margins of error of our calculations. Furthermore, these mutations lead to similar destabilizations of the resulting sulfurane (**IC1**) from −52.1 kJ mol^{-1} (with respect to **RC**) to −21.0 and 22.4 kJ mol^{-1}, respectively. The subsequent sulfonium intermediates (**IC2**) are also destabilized, although now with a marked difference in magnitude between the two mutations, as indicated by the increase in its relative energy from −53.7 kJ mol^{-1} (wild type) to −51.8 kJ mol^{-1} (Y92F) and −28.7 kJ mol^{-1} (Y44F). It is noted that this change in the relative energies of the subsequent sulfonium intermediates has little effect on the barrier for the transfer of a proton from the remaining tyrosyl to the sulfurane's oxygen. For instance, in the wild-type system, the barrier for reaction via **TS2**$_a$ is 0.9 kJ mol^{-1}, while in Y92F and Y44F, it is 0.8 and 3.0 kJ mol^{-1}, respectively. Importantly, however, assuming that the tyrosyls have no effect on the activation of Cys13 (transfer of a proton from Cys13-SH via a H_2O to Glu52COO^-), the rate-limiting step in the reductase stage remains formation of the sulfurane from **RC** (see Figure S4 of the Supporting Information).

The results described above may also provide insight into observations from experimental[22] mutagenesis studies in which the substitution of Tyr92 or Tyr44 (Tyr134 or Tyr82 in *N. meningitidis*) with Phe was shown to have little effect on the catalytic rate. In particular, the experimentally measured difference in rates between the two mutations corresponded to a difference in rate-limiting barrier heights of ∼6 kJ mol^{-1}. The results of this study emphasize the ability of either active

dx.doi.org/10.1021/bi301168p | *Biochemistry* 2013, 52, 1814−1827

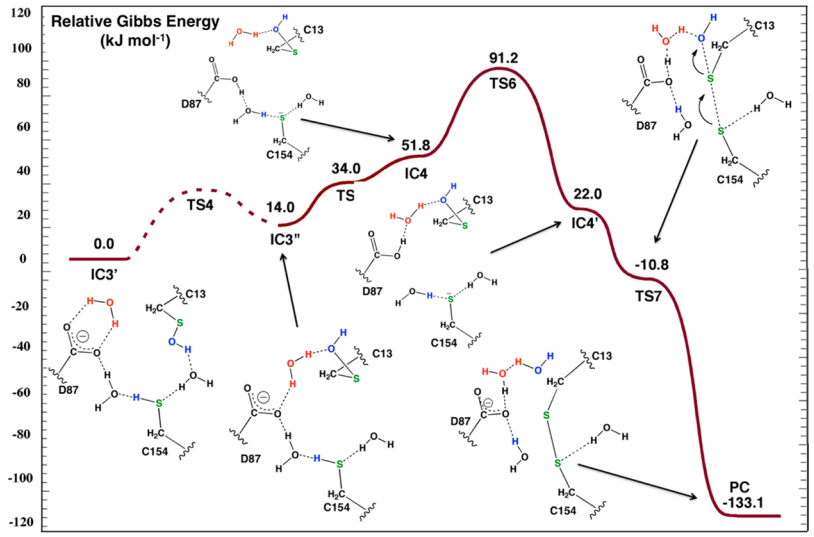

Figure 6. Free energy surface obtained (see Computational Methods) for the reduction of the sulfenic acid-containing complex to give an intramolecular disulfide bond with formation of H_2O.

site tyrosyl to act as a mechanistic acid. Furthermore, they also suggest only minor changes within the margins of error of these calculations in the thermodynamics of formation of the enzyme−sulfenic acid intermediate upon mutation of either tyrosyl.

It should be noted that alternative mechanistic pathways were also considered. In particular, the direct nucleophilic attack of the sulfur of the recycling cysteine (Cys154) at the catalytic cysteine's (Cys13) sulfur center was investigated. That is, the direct reaction of the sulfonium intermediate to give the final product complex (**PC**) bound Met with formation of an intramolecular Cys13S−SCys154 disulfide bond (see Scheme 1B), without formation of a sulfenic acid intermediate (see below). Previous computational studies have shown that if a thiolate is suitably positioned it can readily react with a sulfonium to give a disulfide, e.g., CysS−CysS, and an alkylated sulfide, e.g., Met.[56] However, in sulfonium complexes **IC2**$_a$ and **IC2**$_b$, the sulfurs of the two active site cysteinyl residues are at least 5.1 Å apart, with a Cys13C$_\alpha$—C$_\alpha$Cys154 distance of 7.14 Å. Thus, direct nucleophilic attack of the thiol of Cys154 at the Cys13S center in either sulfonium complex appears unlikely to occur. It is noted that larger distances between the catalytic and recycling cysteines have been observed in the X-ray crystal structures of MsrA's from several species. For example, for an MsrA from *E. coli*, the distance between the C$_\alpha$ atoms of the catalytic and recycling cysteinyl residues is approximately 11.0 Å![37] However, if the Cys13S−S$_{sub}$ bond was first cleaved, Cys13 would then be free to undergo a conformational change that reorients its sulfur closer to that of the recycling cysteine.

Reduction of the Sulfenic Acid with Formation of an Intramolecular Disulfide Bond. As noted for both of the **IC3** complexes described above (**IC3**$_a$ and **IC3**$_b$), the initial Met-O substrate has now been reduced to Met. Importantly, however, with cleavage of the sulfonium's Cys13S−S$_{sub}$ bond and formation of the sulfenic acid Cys13SOH, the Met moiety is now free to leave the active site. This would likely allow water(s) to enter the active site and the anionic tyrosyl residue (Tyr44 or Tyr92) to regain a proton and may result in some changes in the hydrogen bonding network and possibly some repositioning of the active site residues. Hence, as detailed in Computational Methods, to improve our modeling of such changes, we performed an MD simulation on a "resolvated Met-free" Cys13SOH-containing active site complex. The QM/MM-optimized structure obtained at the same level of theory used above, and hereafter termed **IC3′**, is shown in Figure 7.

In **IC3′**, both Tyr92 and Tyr44 are modeled as neutral while the R -group carboxylate of Asp87 is modeled as anionic. That is, the two former residues have regained or kept their proton, while the latter has been deprotonated. It is noted that in both the average structure obtained from MD simulations and in the QM/MM-optimized structure, a chain of waters was observed to interconnect the R groups of Asp87 and the two tyrosyl residues. It thus appears to be possible that regeneration of the neutral tyrosyl residues could occur via the transfer of a proton along a water chain from the Asp87COOH moiety generated during or possibly after sulfenic acid formation (Figure S3 of the Supporting Information).

Structurally, in **IC3′**, the hydroxyl of the Cys13SOH sulfenic acid acts as a hydrogen bond donor to an active site H_2O that is itself simultaneously hydrogen bonded to the backbone carbonyl oxygen of Cys13, the R group imidazole of His155, and the sulfur of Cys154. The thiol of Cys154 is also hydrogen bonded via another water molecule to the R group carboxylate of Asp87. In part because of this hydrogen bond network arrangement, the hydroxyl of the Cys13SOH moiety sits approximately between the sulfurs of Cys13 and Cys154. Consequently, these two mechanistically important sulfur centers are not suitably positioned for the required nucleophilic attack of the Cys154S center at the sulfenic's acid sulfur to form an intramolecular Cys154S−SCys13 disulfide bond. Therefore, a rotation about the C−SOH bond of Cys13SOH (i.e., a change in its C$_\alpha$−C$_\beta$−S−O dihedral angle) with a slight alteration of the active site hydrogen bonding network is required to suitably position the sulfurs of Cys13S and Cys154 for further reaction. More specifically, a change in the C$_\alpha$−C$_\beta$−S−O dihedral angle from 243.9° to 110.0° leads to formation of the alternate conformer **IC3″** lying just slightly higher in energy than **IC3′** by 14.0 kJ mol^{-1} (Figure 6). As can be seen in Figure 7, in **IC3″** the Cys13SOH hydroxyl now acts as a hydrogen bond donor with a water that is itself hydrogen-bonded to the R group carboxylate of Asp87. That is, the sulfenic acid is no longer hydrogen bonded via a water molecule with the thiol of

dx.doi.org/10.1021/bi301168p | *Biochemistry* 2013, 52, 1814−1827

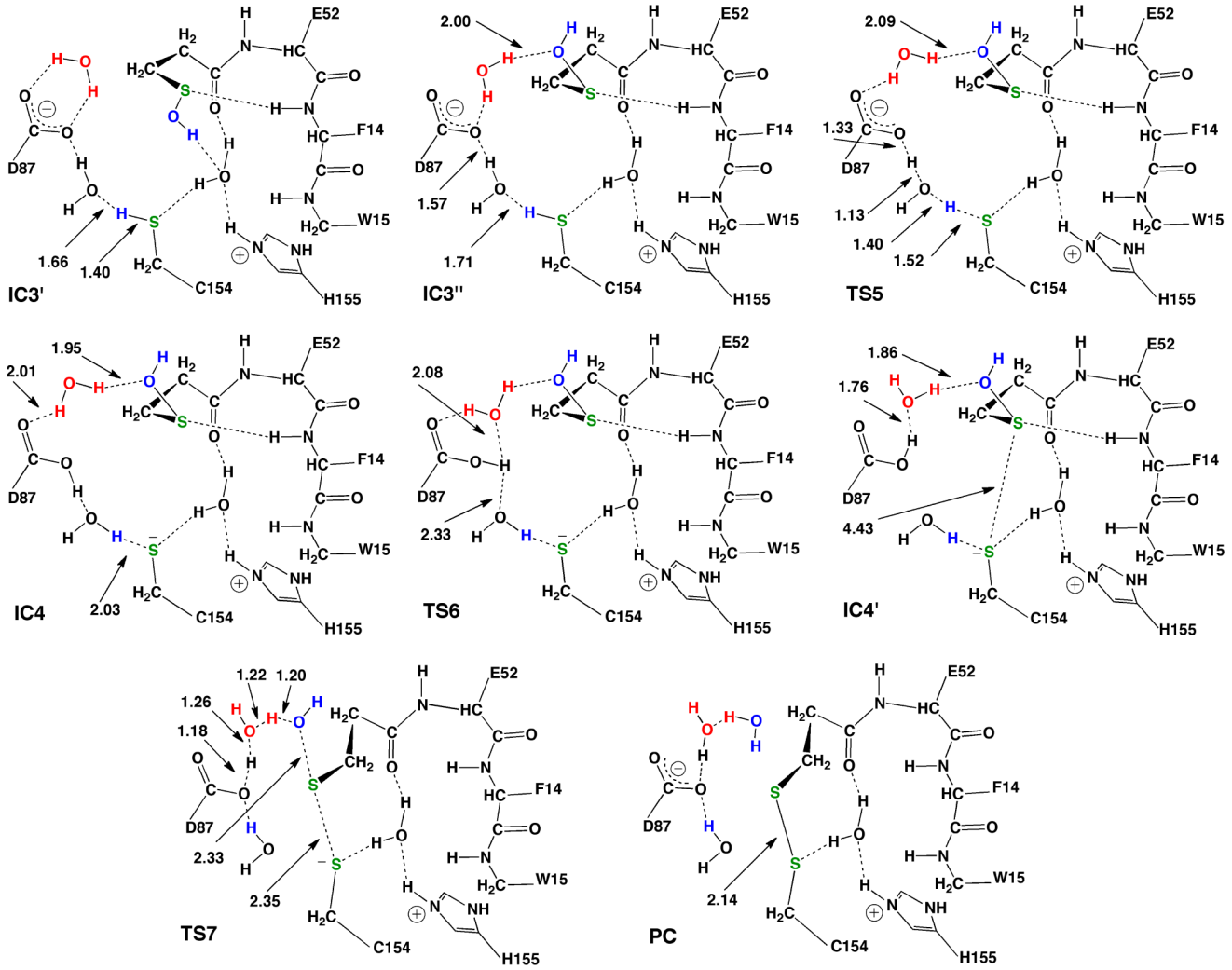

Figure 7. Schematic illustration of the optimized structures for sulfenic acid reduction and formation of a disulfide bond.

Cys154. Importantly, as a result of this rotation, the sulfurs of the catalytic and recycling cysteine are now better positioned with respect to each other for reaction and are closer than in **IC3′** by 0.39 Å with a Cys154S···SCys13 distance of 4.54 Å. Furthermore, the sulfenic acid S−OH bond has become slightly longer, increasing from 1.69 Å (**IC3′**) to 1.72 Å. Unfortunately, within the computational model presented here, we were unable to optimize a transition structure (**TS4**) for interconversion of **IC3′** and **IC3″**. However, for isolated ethanesulfenic acid (CH_3CH_2SOH) at the B3LYP/6-31G(d) level of theory, the analogous rotational barrier is very low at ∼4.0 kJ mol^{-1}. Thus, while the active site sterics and the hydrogen bond network may increase the barrier for this step, it is still unlikely to be significant or rate-limiting. It is also important to note that the sulfenic acid orientation in **IC3″** is in agreement with a sulfenic acid-containing X-ray crystal structure of MsrA from *N. meningitidis* (PDB entry 3BQG).[33] Furthermore, two water molecules were also found to be positioned in the crystal structure such that they may be able to form a hydrogen bond bridge between the sulfenic acid's −SOH oxygen atom and a carboxylate oxygen of Asp87. In addition, a third water molecule was positioned such that it may form a hydrogen bond bridge between the sulfenic acid's sulfur and the R group of His155. However, the X-ray crystal structure as well as our MD structure also shows a chain of waters connecting the sulfenic acid oxygen to Glu52, Tyr44, and Tyr92, suggesting the possibility that one or more of these residues might also be able to play a role as a proton donor in the disulfide formation step.

The nucleophilicity of the Cys154S sulfur center, and hence its ability to attack at the sulfur of Cys13, would be facilitated by deprotonation of the Cys154 thiol. In this computational model, this can be achieved by the transfer of a proton from Cys154SH via a water molecule onto the R group carboxylate of Asp87. This step proceeds via **TS5** to give the $Cys154S^-$ thiolate-containing complex **IC4** just 37.8 kJ mol^{-1} higher in energy than **IC3″**. In **IC4**, the Asp87COOH group remains hydrogen bonded via a water with the $Cys154S^-$ thiolate while the Cys154S···SCys13 distance has decreased further by 0.13 Å, to 4.41 Å (Figure 6). The slightly lower relative energy of **TS5** (17.8 kJ mol^{-1}) with respect to that of **IC4** is an artifact of the use of single-point energy calculations and free energy corrections. It indicates that the reverse reaction, i.e., transfer of a proton from Asp87COOH via a water to $Cys154S^-$, occurs without a barrier.

For the hydroxyl of the sulfenic acid to be a better leaving group for disulfide bond formation, it needs to gain a proton at some point and become H_2O. The now neutralized Asp87 residue could act as a suitable proton donor. In particular, it needs to act as a hydrogen bond donor either directly or

dx.doi.org/10.1021/bi301168p | *Biochemistry* 2013, 52, 1814−1827

indirectly (e.g., via water) with the Cys13SOH oxygen center. This can be achieved by rotation of its carboxylate's −OH moiety, i.e., rotation about the aspartyl's C_β−OH bond, such that it no longer hydrogen bonds indirectly with $Cys154S^-$. This step proceeds via **TS6** with a barrier of 39.4 kJ mol^{-1} with respect to **IC4**. This is only slightly higher by 28.0 kJ mol^{-1} than that obtained for the analogous rotation in isolated propanoic acid at the B3LYP/6-31G(d) level of theory. This likely reflects in part general effects of the active site and the cleaving of the negatively charged Asp87COO-H···OH_2···$^-$SCys154 hydrogen bonding interaction. The resulting alternate conformer that is formed, complex **IC4′**, is 29.8 kJ mol^{-1} lower in energy than **IC4**. The Cys154S···SCys13 distance is only marginally affected by this rotation being 4.43 Å in **IC4′**, while the sulfenic acids S−OH bond has become marginally longer, 1.74 Å (Figure 7).

The final step of the overall mechanism is nucleophilic attack of the anionic sulfur of Cys154 at the sulfur center of the Cys13SOH sulfenic acid to give a Cys154S−SCys13 disulfide bond and proceeds via **TS7**. As illustrated in Figure 7, formation of the disulfide bond occurs with concomitant transfer of the proton from Asp87COOH via a bridging water to the leaving −OH group of the sulfenic acid to give a H_2O molecule. It is noted that this reaction has been computationally investigated previously using density functional theory in combination with small chemical models.[56] Similar to the results presented here, it was also found that disulfide bond formation involved an S_N2 mechanism in which S−S bond formation occurred with concomitant transfer of a proton onto the leaving −OH group.[56] Within this extensive QM/MM approach, however, the relative energy of **TS7** is lower than that of **IC4′** (Figure 6). This suggests that upon rearrangement of the Asp87COOH···OH_2···HOSCys13 hydrogen bond network within the active site environment of MsrA, the reduction of the sulfenic acid to give a disulfide bond can effectively occur without a barrier. The resulting final product complex (**PC**) that is formed is considerably lower in energy than **IC3′** by 133.1 kJ mol^{-1}. The overall highly exothermic mechanism for sulfenic acid formation and its subsequent reduction supports the common experimental observation of the high reactivity of sulfenic acid and challenges in detecting its occurrence in the presence of the recycling cysteine.

It is noted that within this computational model the rate-limiting step of the overall mechanism appears to occur after formation of the sulfenic acid and corresponds to rotation within the Asp87COOH moiety.[57] However, this approach is necessarily "static" and does not include free energy corrections. In contrast, the hydrogen bond network within the active site is likely quite dynamic. Thus, our calculated results for this stage of the overall mechanism likely represent an upper thermodynamic value. Indeed, the approximate rate-limiting barrier obtained from experimental kinetic studies of the wild-type enzyme in the absence of Trx is 56.6 kJ mol^{-1}.[30] This is in good agreement with the rate-limiting barriers presently calculated for the two possible pathways for formation of sulfenic acid (**IC3**) from **PRC**: 61.1 and 85.6 kJ mol^{-1} in the case of Tyr92 and Tyr44 acting as the second mechanistic acid, respectively.

In the mechanism described above for sulfenic acid reduction after methionine formation, the active site model used began with an initially anionic Asp87 (i.e., $Asp87COO^-$) and protonated His155 (i.e., His155-H^+). That is, these residues were in their usual charge states at pH 7. Experimentally, Gand et al.[58] have examined the kinetic effects of mutating either Asp87 or His155 and concluded that a main role of Asp87 is in substrate binding. The MD simulations described above of the prereactive complex are in agreement as suggested by the observation of a consistent direct interaction between Asp87 and the substrate. However, the results of Gand et al. also found that mutating either Asp87 or His155 had similar kinetic effects.[58] We examined the effect of mutating Asp87 to alanine. More specifically, we replaced Asp87 with Ala in the prereactive complex ($\mathbf{PRC}_{Asp87Ala}$) and then resolvated the complex using the same procedure detailed in Computational Methods. This was followed by a 1 ns MD simulation, and the results obtained were analyzed via cluster analysis. Notably, it was observed that in $\mathbf{PRC}_{Asp87Ala}$ the thiol of Cys154 consistently hydrogen bonds to the imidazole of His155 either directly or via a water molecule (see Figure S8 of the Supporting Information). This suggests the possibility of a Cys154 activation pathway involving His155 that is analogous to that we have previously described involving Asp87. Hence, for completeness and given that the pK_a of the R group of His lies near 7 and can be modified by the environment, we also considered an alternate mechanism in which the imidazole of His155 is neutral and thus able to act as a base. For this mechanism, the R group of Asp87 was modeled as neutral as it could still have participated in sulfenic acid formation by accepting a proton from Cys154SH. It should be noted that in the case of His155 facilitating Cys154 activation, no rotation of the hydroxyl in Asp87COOH would be necessary (i.e., **IC4** → **IC4′**). Importantly, His155 was indeed able to act as a base and accept a proton from the thiol of Cys154 in the activation of the latter residue (i.e., **IC3′** → **IC4**) with a calculated reaction barrier of 65.1 kJ mol^{-1} (Table S1 of the Supporting Information). While this is enzymatically feasible, it is higher than obtained for the mechanism described above via **TS5**. This suggests that mutation of Asp87 may not significantly affect sulfenic acid reduction as either basic residue near the thiol of the recycling cysteine could potentially facilitate its activation.

CONCLUSION

The overall mechanism(s) by which methionine sulfoxide reductase A (MsrA) from *M. tuberculosis* catalyzes the reduction of *S*-methionine sulfoxide (Met-O) to methionine (Met), i.e., the reductase stage, has been investigated via the complementary application of docking, molecular dynamics (MD) simulations, and ONIOM (QM/MM) calculations. More specifically, docking and MD simulation were used to obtain solvated structures for the initial active site-bound substrate complex in which the catalytic cysteine (Cys13SH) is not yet activated (**PRC**), i.e., neutral. An ONIOM QM/MM approach in combination with a large active site model has been used to examine the mechanism of Cys13 activation and subsequent pathway(s) leading to formation of a sulfenic acid intermediate. In particular, Cys13SH is able to transfer its proton via a bridging water molecule onto the R group carboxylate of the active site glutamate (Glu52) with a modest energy cost of 49.3 kJ mol^{-1}, to give the activated active site-bound substrate complex, **RC**. The now anionic $Cys13S^-$ sulfur then nucleophilically attacks the sulfur of the Met-O substrate. This occurs with concomitant transfer of a proton from the now neutral Glu52COOH group onto the substrate sulfoxide oxygen. The resulting sulfurane intermediate is "polarized" by the active site environment. Consequently, the sulfurane's oxygen can readily accept a proton from the phenol hydroxyl of

either of the active site tyrosyl residues, Tyr44 and Tyr92, with a negligible barrier or without a barrier, to give a sulfonium cation and water. The water formed is hydrogen bonded to the R groups of both active site Tyr44 and Tyr92, and Glu52.

It was found that a water moiety was then able to directly and readily attack the sulfonium cation at its Cys13S center, i.e., the sulfur of the catalytic cysteine, to give a sulfenic acid Cys13SOH and methionine in one step. In the active site chemical model used, the recycling cysteine (Cys154) was neutral, i.e., Cys154SH. It is found that a neutral Cys154SH group is able to facilitate sulfenic acid formation by accepting a proton from the attacking H_2O while simultaneously transferring its proton via a water to the nearby R group carboxylate of Asp87. For the case in which Tyr92 acted as the second mechanistic acid, this step occurs with a barrier of 32.6 kJ mol^{-1}, while for the alternate case in which Tyr44 acted as an acid, the barrier is higher but still enzymatically feasible at 85.6 kJ mol^{-1}. The resulting sulfenic acid intermediate complexes formed, **IC3$_a$** and **IC3$_b$**, respectively, are calculated to have significantly lower energies than RC by −222.4 and −208.3 kJ mol^{-1}, respectively.

Reduction of the sulfenic acid to give an intramolecular Cys154S−SCys13 disulfide bond, with formation of H_2O, was found to occur via series of low-barrier steps. Primarily, these steps involve the rearrangement of the active site hydrogen bond network and suitable positioning of the sulfur centers of Cys154 and Cys13 for reaction. It is found that nucleophilic attack by the sulfur of the neutral thiol of Cys154SH is facilitated by the R group carboxylate of Asp87. In particular, the latter is able to accept the thiol proton and then transfer it via a H_2O onto the leaving −OH group of sulfenic acid (Cys13SOH) concomitant with formation of the disulfide bond. Further, our results suggest an S_N2 mechanism for disulfide bond formation, and that it would happen spontaneously after activation of Cys154 and suitable positioning of the Cys13SOH sulfur for nucleophilic attack by the thiolate sulfur of Cys154.

Thus, these results also suggest that both active site cysteines can at least initially be neutral. During the course of the reaction, they can be activated for formation of the sulfurane or reduction of the sulfenic acid via direct or indirect proton transfers to, for instance, the R groups of some active site residues, including Glu52 and Asp87.

■ ASSOCIATED CONTENT

Supporting Information

Cartesian coordinates and energies of the optimized structures reported here. This material is available free of charge via the Internet at http://pubs.acs.org.

■ AUTHOR INFORMATION

Corresponding Author

*E-mail: gauld@uwindsor.ca. Telephone: (519) 253-3000, ext. 3992. Fax: (519) 973-7098.

Funding

This work was supported by grants from the Natural Sciences and Engineering Research Council of Canada (NSERC).

Notes

The authors declare no competing financial interest.

■ ACKNOWLEDGMENTS

We thank SHARCNET for additional computational resources.

■ REFERENCES

(1) Stadtman, E. R., Moskovitz, J., and Levine, R. L. (2003) Oxidation of methionine residues of proteins: Biological consequences. *Antioxid. Redox Signaling 5*, 577−582.

(2) Koc, A., and Gladyshev, V. N. (2007) Methionine sulfoxide reduction and the aging process. In *Biogerontology: Mechanisms and interventions* (Rattan, S. I. S., and Akman, S., Eds.) pp 383−386, Blackwell Publishing, Oxford, U.K.

(3) Levine, R. L., Moskovitz, J., and Stadtman, E. R. (2000) Oxidation of methionine in proteins: Roles in antioxidant defense and cellular regulation. *IUBMB Life 50*, 301−307.

(4) Levine, R. L., Mosoni, L., Berlett, B. S., and Stadtman, E. R. (1996) Methionine residues as endogenous antioxidants in proteins. *Proc. Natl. Acad. Sci. U.S.A. 93*, 15036−15040.

(5) Levine, R. L., Berlett, B. S., Moskovitz, J., Mosoni, L., and Stadtman, E. R. (1999) Methionine residues may protect proteins from critical oxidative damage. *Mech. Ageing Dev. 107*, 323−332.

(6) Agbas, A., and Moskovitz, J. (2009) The role of methionine oxidation/reduction in the regulation of immune response. *Curr. Signal Transduction Ther. 4*, 46−50.

(7) Haenold, R., Wassef, D. M., Heinemann, S. H., and Hoshi, T. (2005) Oxidative damage, aging and anti-aging strategies. *Age 27*, 183−199.

(8) Stadtman, E. R. (2004) Role of oxidant species in aging. *Curr. Med. Chem. 11*, 1105−1112.

(9) Schöneich, C. (2005) Methionine oxidation by reactive oxygen species: Reaction mechanisms and relevance to Alzheimer's disease. *Biochim. Biophys. Acta 1703*, 111−119.

(10) Ezraty, B., Aussel, L., and Barras, F. (2005) Methionine sulfoxide reductases in prokaryotes. *Biochim. Biophys. Acta 1703*, 221−229.

(11) Weissbach, H., Resnick, L., and Brot, N. (2005) Methionine sulfoxide reductase: History and cellular role in protecting against oxidative damage. *Biochim. Biophys. Acta 1703*, 203−212.

(12) Trachootham, D., Lu, W. Q., Ogasawara, M. A., Valle, N. R. D., and Huang, P. (2008) Redox regulation of cell survival. *Antioxid. Redox Signaling 10*, 1343−1374.

(13) Moskovitz, J. (2005) Methionine sulfoxide reductases: Ubiquitous enzymes involved in antioxidant defense, protein regulation, and prevention of aging-associated diseases. *Biochim. Biophys. Acta 1703*, 213−219.

(14) Lowther, W. T., Brot, N., Weissbach, H., and Matthews, B. W. (2000) Structure and mechanism of peptide methionine sulfoxide reductase, an "anti-oxidation" enzyme. *Biochemistry 39*, 13307−13312.

(15) Chen, B. W., Markillie, L. M., Xiong, Y. J., Mayer, M. U., and Squier, T. C. (2007) Increased catalytic efficiency following gene fusion of bifunctional methionine sulfoxide reductase enzymes from *Shewanella oneidensis*. *Biochemistry 46*, 14153−14161.

(16) Kim, Y. K., Shin, Y. J., Lee, W. H., Kim, H. Y., and Hwang, K. Y. (2009) Structural and kinetic analysis of an MsrA-MsrB fusion protein from *Streptococcus pneumoniae*. *Mol. Microbiol. 72*, 699−709.

(17) Moskovitz, J., Maiti, P., Lopes, D. H. J., Oien, D. B., Attar, A., Liu, T. Y., Mittal, S., Hayes, J., and Bitan, G. (2011) Induction of methionine-sulfoxide reductases protects neurons from amyloid β-protein insults in vitro and in vivo. *Biochemistry 50*, 10687−10697.

(18) Lim, J. C., You, Z., Kim, G., and Levine, R. L. (2011) Methionine sulfoxide reductase A is a stereospecific methionine oxidase. *Proc. Natl. Acad. Sci. U.S.A. 108*, 10472−10477.

(19) Boschi-Muller, S., Gand, A., and Branlant, G. (2008) The methionine sulfoxide reductases: Catalysis and substrate specificities. *Arch. Biochem. Biophys. 474*, 266−273.

(20) Lowther, W. T., Weissbach, H., Etienne, F., Brot, N., and Matthews, B. W. (2002) The mirrored methionine sulfoxide reductases of *Neisseria gonorrheae* pilB. *Nat. Struct. Biol. 9*, 348−352.

(21) Neiers, F., Sonkaria, S., Olry, A., Boschi-Muller, S., and Branlant, G. (2007) Characterization of the amino acids from *Neisseria meningitidis* methionine sulfoxide reductase B involved in the chemical catalysis and substrate specificity of the reductase step. *J. Biol. Chem. 282*, 32397−32405.

(22) Antoine, M., Gand, A., Boschi-Muller, S., and Branlant, G. (2006) Characterization of the amino acids from *Neisseria meningitidis* MsrA involved in the chemical catalysis of the methionine sulfoxide reduction step. *J. Biol. Chem. 281*, 39062−39070.
(23) Singh, V. K., and Moskovitz, J. (2003) Multiple methionine sulfoxide reductase genes in *Staphylococcus aureus*: Expression of activity and roles in tolerance of oxidative stress. *Microbiology (Reading, U.K.) 149*, 2739−2747.
(24) Douglas, T., Daniel, D. S., Parida, B. K., Jagannath, C., and Dhandayuthapani, S. (2004) Methionine sulfoxide reductase A (MsrA) deficiency affects the survival of *Mycobacterium smegmatis* within macrophages. *J. Bacteriol. 186*, 3590−3598.
(25) Nan, C. L., Li, Y. J., Jean-Charles, P. Y., Chen, G. Z., Kreymerman, A., Prentice, H., Weissbach, H., and Huang, X. P. (2010) Deficiency of methionine sulfoxide reductase A causes cellular dysfunction and mitochondrial damage in cardiac myocytes under physical and oxidative stresses. *Biochem. Biophys. Res. Commun. 402*, 608−613.
(26) Ruan, H., Tang, X. D., Chen, M. L., Joiner, M. A., Sun, G., Brot, N., Weissbach, H., Heinemann, S. H., Iverson, L., Wu, C. F., and Hoshi, T. (2002) High-quality life extension by the enzyme peptide methionine sulfoxide reductase. *Proc. Natl. Acad. Sci. U.S.A. 99*, 2748−2753.
(27) Moskovitz, J., Bar-Noy, S., Williams, W. M., Berlett, B. S., and Stadtman, E. R. (2001) Methionine sulfoxide reductase (MsrA) is a regulator of antioxidant defense and lifespan in mammals. *Proc. Natl. Acad. Sci. U.S.A. 98*, 12920−12925.
(28) De Luca, A., Sanna, F., Sallese, M., Ruggiero, C., Grossi, M., Sacchetta, P., Rossi, C., De Laurenzi, V., Di Ilio, C., and Favaloro, B. (2010) Methionine sulfoxide reductase A down-regulation in human breast cancer cells results in a more aggressive phenotype. *Proc. Natl. Acad. Sci. U.S.A. 107*, 18628−18633.
(29) Boschi-Muller, S., Azza, S., Sanglier-Cianferani, S., Talfournier, F., Van Dorsselear, A., and Branlant, G. (2000) A sulfenic acid enzyme intermdiate is involved in the catalytic mechanism of peptide methionine sulfoxide reductase from *Escherichia coli*. *J. Biol. Chem. 275*, 35908−35913.
(30) Antione, M., Boschi-Muller, S., and Branlant, G. (2003) Kinetic characterization of the chemical steps involved in the catalytic mechanism of methionine sulfoxide reductase A from *Neisseria meningitidis*. *J. Biol. Chem. 278*, 45352−45357.
(31) Lowther, W. T., Brot, N., Weissbach, H., Honek, J. F., and Matthews, B. W. (2000) Thiol-disulfide exchange is involved in the catalytic mechanism of peptide methionine sulfoxide reductase. *Proc. Natl. Acad. Sci. U.S.A. 97*, 6463−6468.
(32) Boschi-Muller, S., Olry, A., Antoine, M., and Branlant, G. (2005) The enzymology and biochemistry of methionine sulfoxide reductases. *Biochim. Biophys. Acta 1703*, 231−238.
(33) Ranaivoson, F. M., Antoine, M., Kauffmann, B., Bosch-Muller, S., Aubry, A., Branlant, G., and Favier, F. (2008) A structural analysis of the catalytic mechanism of methionine sulfoxide reductase a from *Neisseria meningitidis*. *J. Mol. Biol. 377*, 268−280.
(34) Thiriot, E., Monard, G., Boschi-Muller, S., Branlant, G., and Ruiz-Lopez, M. F. (2011) Reduction mechanism in class A methionine sulfoxide reductases: A theoretical chemistry investigation. *Theor. Chem. Acc. 129*, 93−103.
(35) (a) Robinet, J. J., Dokainish, H. M., Paterson, D. J., and Gauld, J. W. (2011) A sulfonium cation intermediate in the mechanism of methionine sulfoxide reductase B: A DFT study. *J. Phys. Chem. B 115*, 9202−9212. (b) Neiers, F., Boschi-Muller, S., and Branlant, G. (2011) Comment on "A Sulfonium Cation Intermediate in the Mechanism of Methionine Sulfoxide Reductase B: A DFT Study". *J. Phys. Chem. B 115*, 10775−10775. (c) Robinet, J. J., Dokainish, H. M., Paterson, D. J., and Gauld, J. W. (2011) Reply to the "Comment on 'A Sulfonium Cation Intermediate in the Mechanism of Methionine Sulfoxide Reductase B: A DFT Study'". *J. Phys. Chem. B 115*, 10776−10777.
(36) *MOE*, version 2009.10 (2009) Chemical Computing Group Inc., Montreal.
(37) Taylor, A. B., Benglis, D. M., Dhandayuthapani, S., and Hart, P. J. (2003) Structure of *Mycobacterium tuberculosis* methionine sulfoxide reductase A in complex with protein-bound methionine. *J. Bacteriol. 185*, 4119−4126.
(38) Bushnell, E. A. C., Erdtman, E., Llano, J., Eriksson, L. A., and Gauld, J. W. (2010) The first branching point in porphyrin biosynthesis: A systematic docking, molecular dynamics and quantum mechanical/molecular mechanical study of substrate binding and mechanism of uroporphyrinogen-III decarboxylase. *J. Comput. Chem. 32*, 822−834.
(39) Wang, J. M., Wolf, R. M., Caldwell, J. W., Kollman, P. A., and Case, D. A. (2004) Development and testing of a general Amber force field. *J. Comput. Chem. 25*, 1157−1174.
(40) Bushnell, E. A. C., Huang, W., Llano, J., and Gauld, J. W. (2012) Molecular dynamics investigation into substrate binding and identity of the catalytic base in the mechanism of threonyl-tRNA synthetase. *J. Phys. Chem. B 116*, 5205−5212.
(41) Svensson, M., Humbel, S., Froese, R. D. J., Matsubara, T., Sieber, S., and Morokuma, K. (1996) ONIOM: A multilayered integrated MO+MM method for geometry optimizations and single point energy predictions. A test for Diels-Alder reactions and Pt(P(t-Bu)$_3$)$_2$ + H-2 oxidative addition. *J. Phys. Chem. 100*, 19357−19363.
(42) Frisch, M. J., Trucks, G. W., Schlegel, H. B., Scuseria, G. E., Robb, M. A., Cheeseman, J. R., Scalmani, G., Barone, V., Mennucci, B., Petersson, G. A., Nakatsuji, H., Caricato, M., Li, X., Hratchian, H. P., Izmaylov, A. F., Bloino, J., Zheng, G., Sonnenberg, J. L., Hada, M., Ehara, M., Toyota, K., Fukuda, R., Hasegawa, J., Ishida, M., Nakajima, T., Honda, Y., Kitao, O., Nakai, H., Vreven, T., Montgomery, J. A., Jr., Peralta, J. E., Ogliaro, F., Bearpark, M., Heyd, J. J., Brothers, E., Kudin, K. N., Staroverov, V. N., Kobayashi, R., Normand, J., Raghavachari, K., Rendell, A., Burant, J. C., Iyengar, S. S., Tomasi, J., Cossi, M., Rega, N., Millam, N. J., Klene, M., Knox, J. E., Cross, J. B., Bakken, V., Adamo, C., Jaramillo, J., Gomperts, R., Stratmann, R. E., Yazyev, O., Austin, A. J., Cammi, R., Pomelli, C., Ochterski, J. W., Martin, R. L., Morokuma, K., Zakrzewski, V. G., Voth, G. A., Salvador, P., Dannenberg, J. J., Dapprich, S., Daniels, A. D., Farkas, Ö., Foresman, J. B., Ortiz, J. V., Cioslowski, J., and Fox, D. J. (2009) *Gaussian 09*, Gaussian Inc., Wallingford, CT.
(43) Becke, A. D. (1993) A new mixing of Hartree-Fock and local density-functional theories. *J. Chem. Phys. 98*, 1372−1377.
(44) Lee, C., Yang, W., and Parr, R. G. (1988) Development of the Colle-Salvetti correlation-energy formula into a functional of the electron density. *Phys. Rev. B 37*, 785−789.
(45) Cornell, W. D., Cieplak, P., Bayly, C. I., Gould, I. R., Merz, K. M., Ferguson, D. M., Spellmeyer, D. C., Fox, T., Caldwell, J. W., and Kollman, P. A. (1996) A second generation force field for the simulation of proteins, nucleic acids, and organic molecules (vol 117, pg 5179, 1995). *J. Am. Chem. Soc. 118*, 2309.
(46) Lodola, A., Sirirak, J., Fey, N., Rivara, S., Mor, M., and Mulholland, A. J. (2010) Structural fluctuations in enzyme-catalyzed reactions: Determinants of reactivity in fatty acid amide hydrolase from multivariate statistical analysis of quantum mechanics/molecular mechanics paths. *J. Chem. Theory Comput. 6*, 2948−2960.
(47) Xu, Q., Li, L. Y., and Guo, H. (2010) Understanding the mechanism of deacylation reaction catalyzed by the serine carboxyl peptidase Kumamolisin-As: Insights from QM/MM free energy simulations. *J. Phys. Chem. B 114*, 10594−10600.
(48) Xiao, C., and Zhang, Y. (2007) Catalytic mechanism and metal specificity of bacterial peptide deformylase: A density functional QM/MM study. *J. Phys. Chem. B 111*, 6229−6235.
(49) Llano, J., and Gauld, J. W. (2010) Mechanistics of enzyme catalysis: From small to large active-site models. In *Quantum biochemistry: Electronic structure and biological activity* (Matta, C. F., Ed.) p 643, Wiley-VCH, Weinheim, Germany.
(50) Sousa, S. F., Fernandes, P. A., and Ramos, M. J. (2012) Computational enzymatic catalysis: Clarifying enzymatic mechanisms with the help of computers. *Phys. Chem. Chem. Phys. 14*, 12431−12441.

(51) Przybylski, J. L., and Wetmore, S. D. (2011) A QM/QM Investigation of the hUNG2 Reaction Surface: The Untold Tale of a Catalytic Residue. *Biochemistry 50*, 4218−4227.
(52) Tian, B. X., Erdtman, E., and Eriksson, L. A. (2012) Catalytic Mechanism of Porphobilinogen Synthase: The Chemical Step Revisited by QM/MM Calculations. *J. Phys. Chem. B 116*, 12105−12112.
(53) Cohen, A. J., Mori-Sanchez, P., and Yang, W. T. (2012) Challenges for Density Functional Theory. *Chem. Rev. 112*, 289−320.
(54) Zhou, P., Tian, F. F., Lv, F. L., and Shang, Z. C. (2009) Geometric characteristics of hydrogen bonds involving sulfur atoms in proteins. *Proteins 76*, 151−163.
(55) Balta, B., Monard, G., Ruiz-Lopez, M. F., Antoine, M., Gand, A., Boschi-Muller, S., and Branlant, G. (2006) Theoretical study of the reduction mechanism of sulfoxides by thiols. *J. Phys. Chem. A 110*, 7628−7636.
(56) Bayse, C. A. (2011) Transition states for cysteine redox processes modeled by DFT and solvent-assisted proton exchange. *Org. Biomol. Chem. 9*, 4748−4751.
(57) Laidler, K. J. (1987) *Chemical kinetics*, 3rd ed., HarperCollins Publishers, New York.
(58) Gand, A., Antoine, M., Boschi-Muller, S., and Branlant, G. (2007) *J. Biol. Chem. 282*, 20484−20491.